

# Preparation of porous aluminium oxide ( $\text{Al}_2\text{O}_3$ ) hollow fibre membranes by a combined phase-inversion and sintering method

Shaomin Liu<sup>a</sup>, K. Li<sup>b,\*</sup>, R. Hughes<sup>c</sup>

<sup>a</sup>*Institute of Environmental Science and Engineering, 18 Nanyang Drive, Singapore 637723, Singapore*

<sup>b</sup>*Department of Chemical Engineering, University of Bath, Bath BA2 7AY, UK*

<sup>c</sup>*Department of Chemical Engineering, University of Salford, Salford M5 4WT, UK*

Received 27 July 2002; received in revised form 28 November 2002; accepted 5 January 2003

## Abstract

$\text{Al}_2\text{O}_3$  hollow fibre membranes were prepared by a combined phase-inversion and sintering method. An organic binder solution (dope) containing suspended aluminium oxide ( $\text{Al}_2\text{O}_3$ ) powders, either in mono size or a distributed size, is spun to a hollow fibre precursor, which is then sintered at elevated temperatures. In spinning the hollow fibre precursor, polyethersulfone (PESf), *N*-methyl-2-pyrrolidone (NMP) and polyvinyl pyrrolidone (PVP) were used as a polymer binder, a solvent and an additive, respectively. The  $\text{Al}_2\text{O}_3$  hollow fibre membranes prepared were characterized using a scanning electron microscope (SEM) and gas permeation techniques. Effects of  $\text{Al}_2\text{O}_3$  particle size and size distribution, the sintering temperature and  $\text{Al}_2\text{O}_3$ /PESf ratio on the structure and performance of the resulting membranes were studied extensively. The prepared  $\text{Al}_2\text{O}_3$  hollow fibre membranes retains its asymmetric structure (mainly resulted from the phase inversion technique) even after the sintering process. Preparation of the  $\text{Al}_2\text{O}_3$  hollow fibre membrane with a high mechanical strength and moderate permeation characteristics is feasible if the  $\text{Al}_2\text{O}_3$  powders with a distributed particle size in the spinning (dope) solution is employed.

© 2003 Elsevier Ltd and Techna S.r.l. All rights reserved.

**Keywords:** D.  $\text{Al}_2\text{O}_3$ ; Hollow fibres; Ceramic membranes

## 1. Introduction

Polymeric hollow fibre membranes are in current use for a number of process applications, including filtration, desalination, gas separation and in membrane reactors. Inorganic membranes have been developed for similar applications, especially where high temperature operation precludes the use of existing polymeric membranes [1,2]. However, currently produced inorganic membranes are usually in the form of flat discs, finite sized tubes with diameters of at least several millimetres or multi-channel monoliths and consequently have low surface area/volume ratios ranged from 30 to 250  $\text{m}^2\cdot\text{m}^{-3}$  [2–4]. These low area/volume ratios compare unfavourably with polymeric hollow fibre modules where area/volume ratios of several thousand are obtainable; this limits the application of current inorganic monolithic,

tubular and disc membranes. This limitation is most evident in catalytic membrane reactors, where it is desirable to maximize the area of the membrane module to increase the permeation rate to remove the product species from the reaction zone [5].

Currently, a few methods have been employed for preparing inorganic hollow fibres, including dry spinning a system of inorganic material and binder [6–9], wet spinning a suitable inorganic material-containing solution and/or sols [10], depositing fibres from the gas phase on to a substrate, or pyrolyzing the polymers [11–13]. Recently, the well-known phase inversion method, commonly employed for spinning polymeric hollow fibre membranes, has been successfully modified to prepare the ceramic hollow fibres [14–16]. Because of the phase inversion characteristics, the prepared inorganic hollow fibres possess an asymmetric structure, which provides a better permeability for a given thickness. Thus, they can be used directly not only in many separation processes, but also to be served as a porous support for composite membrane formation [17].

\* Corresponding author. Tel.: +44-1225-386372; fax: +44-1225-386894.

E-mail address: k.li@bath.ac.uk (K. Li).

Our earlier study [14] was focused on the formation principles and the final resulting membrane structure analysis was only based on the starting solution containing 1- $\mu\text{m}$  of aluminium oxide ( $\text{Al}_2\text{O}_3$ ) powders. Because of complicity of the combined phase-inversion and sintering process, the relationship between the original arrangement of the primary particles/powder size and structure of the final resulting membranes remains unclear and need to be further explored. In this study, the effects of particle size distribution (by controlling of the addition of different weight ratio of 1, 0.3, 0.01  $\mu\text{m}$   $\text{Al}_2\text{O}_3$  particles) of the starting (dope) solution and sintering temperatures on the final resulting membranes and their mechanical strength have been carefully studied. The optimum conditions for fabricating the asymmetric aluminium oxide ( $\text{Al}_2\text{O}_3$ ) hollow fibre membranes were identified. It is hoped that the ceramic hollow fibre membranes would have their niche in chemical reaction/separation, not replacing existing membranes, but rather contributing an added dimension to current capabilities.

## 2. Experimental

### 2.1. Materials

Commercially available aluminium oxide powders with three different particle diameters of 0.01  $\mu\text{m}$  (gamma/alpha, surface area 100  $\text{m}^2/\text{g}$ ), 0.3  $\mu\text{m}$  (gamma/alpha, surface area 15  $\text{m}^2/\text{g}$ ) and 1  $\mu\text{m}$  (alpha, surface area 10  $\text{m}^2/\text{g}$ ) [purchased from Alfa AESAR, A Johnson Matthey company] were used as membrane materials. PESf [Radel A-300, Ameco Performance, USA], and *N*-methyl-2-pyrrolidone (NMP) [Synthesis Grade, Merck] were used for preparing the starting solution. Polyvinylpyrrolidone (PVP, K90) [GAF® ISP Technologies, Inc.  $M_w = 630,000$ ] was used as an additive. Tap water was used as both the internal and external coagulants.

### 2.2. Preparation of the aluminium oxide ( $\text{Al}_2\text{O}_3$ ) hollow fibres

The required quantity of NMP was taken in a 1-l wide-neck reaction flask and the PESf was slowly added over a period of 30 min to form the polymer solution. After the polymer solution was formed, a given amount of aluminium oxide (0.01, 0.3 and 1  $\mu\text{m}$  or a mixture of them) was then added into the polymer solution slowly, while a Heidolph RZR 2000 stirrer was used at a speed of  $\sim 300$  rpm to ensure that all the aluminium oxide powders is dispersed uniformly in the polymer solution. PVP as an additive was also introduced into the solution to modulate its viscosity. Finally, the polymer solution was degassed at room temperature.

The degassed starting (dope) solution containing the dispersed aluminum oxide powders was transferred to a

stainless steel reservoir and pressurized to 20–30 psig using nitrogen. A tube-in-orifice spinneret with orifice diameter/inner diameter of the tube of 2.0/0.72 (mm) was used to obtain hollow fibre precursors. The air-gap was kept at 2 cm for all spinning runs. Finally, the forming hollow fibre precursor was passed through a water bath to complete solidification process and thoroughly washed in water. The details of the spinning equipment and procedure on hollow fibre spinning have been described elsewhere [18].

The formed hollow fibre precursors were first heated in a CARBOLITE furnace at about 500 °C for 2 h to remove the organic polymer binder and then were calcined at a high temperature for about 10 h to allow the fusion and bonding to occur. The calcination temperature used in this study was between 1300 and 1600 °C.

### 2.3. Membrane characterizations

#### 2.3.1. Scanning electron microscopy (SEM)

Structures of the prepared hollow fibre membranes were visually observed using a scanning electron microscope (Jeol JSM-5600). The precursor hollow fibre was first immersed in liquid nitrogen. After about 10 min, the frozen membranes were slowly flexed in the liquid nitrogen until a clear cross-sectional fracture occurred. For the inorganic hollow fibre (after calcination), the clear cross-sectional fracture may be obtained by directly snapping the fibre. These membrane samples were then positioned on a metal holder and gold coated using sputter-coating operated under vacuum. The SEM micrographs of both surface and cross-section of the hollow fibre membranes were taken at various magnifications.

#### 2.3.2. Three point bending test

The mechanical strength of the inorganic hollow fiber membranes was characterised by the values of three point bending strength. The value measurements were performed with Instron Model 5544 tensile tester provided with a load cell for 5 kN. A hollow fiber sample was fixed on the sample holder, which has 6 cm distance. The bending strength,  $\sigma_F$ , was calculated from the following equation

$$\sigma_F = \frac{8FLD}{\pi(D^4 - d^4)},$$

which can be derived from the principles in references [19,20]. Here,  $F$  is the measured force at which fracture take place;  $L$ ,  $D$  and  $d$  are the length (in this case, 6 cm), the outside diameter and the inner side diameter, respectively.

#### 2.3.3. Gas permeation test

The permeabilities of nitrogen through the sintered hollow fibers were measured at 1 atm of the gas pressure

difference in a home-made permeation test cell. Fig. 1 is the experimental setup for the measurement of gas permeability. The operating pressure (1 atm) can be read from the KN2200 electronic pressure gauge. To make the permeation module, one end of the hollow fiber was sealed by the quick-setting epoxy resin, and the other end of the fiber was left open. The nitrogen gas permeability was calculated from the hollow fiber dimensions, permeate flow rate and feed pressure by the following equation:

$$J = \frac{Q \ln(D_o/D_i)}{\pi L(D_o - D_i) \cdot \Delta p}$$

where  $J$ ,  $Q$ ,  $D_o/D_i$ ,  $L$  and  $\Delta p$  are the gas permeability of nitrogen ( $\text{mol/m}^2\text{Pas}$ ), the total  $\text{N}_2$  permeation rate ( $\text{mol/s}$ ), the outside/inside diameter of the hollow fiber (m), the hollow fiber length (m), and the partial pressure difference across the membrane (Pa), respectively.

### 3. Results and discussion

#### 3.1. Morphology study of $\text{Al}_2\text{O}_3$ hollow fibres

SEM micrographs of the  $\text{Al}_2\text{O}_3$  hollow fibre precursors and their sintered fibres, spun from two different dopes with one containing PESf 10%, PVP 0.5%, NMP 39.5%, and 1- $\mu\text{m}$   $\text{Al}_2\text{O}_3$  50% and the other containing PESf 10%, PVP 0.5%, NMP 39.5%, and 0.3- $\mu\text{m}$   $\text{Al}_2\text{O}_3$  50% (wt%) are shown in Figs. 2 and 3, respectively. The sintering process was carried out in air at temperature of 1500 °C. It can be seen from the micrograph of Fig. 2(AI) that the OD and ID of the fibre precursor prepared from 1- $\mu\text{m}$  particles were measured to be 1287 and 847  $\mu\text{m}$  and were shrunk to 1044 and 726  $\mu\text{m}$  [Fig. 2(BI)], respectively. Similarly, Figs. 3(AI) and 3(BI) depict that the OD and ID of the fibre precursor and the sintered fibre prepared from 0.3- $\mu\text{m}$  particles were shrunk from 1705 and 1118  $\mu\text{m}$  to 1333 and 911

$\mu\text{m}$ , respectively. Further comparing the fibre dimensions of the precursors and the sintered ones reveals that the fibres prepared from 0.3- $\mu\text{m}$  particles have a higher shrinkage during the sintering process. This is probably due to the fact that for the same weight of  $\text{Al}_2\text{O}_3$  adding into a given volume of the binder solution, the smaller particle size (0.3  $\mu\text{m}$ ) would leave higher voids compared to the larger particle size (1  $\mu\text{m}$ ). As the voids are generally occupied by the polymer binder, which is ultimately removed during the sintering process, the higher shrinkage of the resulting fibres is, thus, expected for 0.3- $\mu\text{m}$  particles.

Cross-sectional structures of the fibre precursor and the sintered fibre prepared from 1- $\mu\text{m}$  particles are shown in Fig. 2(AII) and (BII). It can be seen from Fig. 2(AII) that near the outer and inner walls of the fibre precursor, long finger-like structures are present and that at centre of the hollow fibre precursor, sponge-like structures are possessed. The appearance of the fibre structures shown in the figure can be attributed to the rapid precipitation occurred at both the inner and outer fibre walls resulting in long fingers and to the slow precipitation giving the sponge-like structure at the centre of the fibre. It is interesting to note that the cross-sectional structure of the fibre precursor is well maintained after the sintering process as shown in Fig. 2(BII). Fig. 3(AII) and (BII) depicts the cross-sectional structures of the fibre precursor and the sintered fibre prepared from 0.3- $\mu\text{m}$  particles. Compared to the fibres prepared from 1- $\mu\text{m}$  particles, it clearly shows that after the sintering, the fibre prepared from 0.3- $\mu\text{m}$  particles is much denser, which probably resulted from the higher shrinkage during the sintering process. Compared to the traditional flat and tubular membranes, the developed  $\text{Al}_2\text{O}_3$  hollow fibre membranes have the advantage of higher surface area/volume ratios. For example, the sintered hollow fibre membranes from Figs. 2(B) and 3(B) have the surface area per membrane volume ratios of 3831 and 3000  $\text{m}^2/\text{m}^3$ , respectively. When these hollow fibre membranes are assembled in the modules, they are very compact and have a practical surface/volume ratio of  $> 1000 \text{ m}^2/\text{m}^3$ .

Fig. 2(AIII) shows the surface of the hollow fibre precursor. It can be seen that the surface of the precursor is similar to the conventional polymeric membranes prepared via the phase inversion technique. Further comparing the SEM photos, especially for the surfaces between the precursors [Figs. 2(AIII) and 3(AIII)] and the sintered fibre [Figs. 2(BIII) and 3(BIII)] reveals that the pore quantity and pore size may have changed after the sintering process although the general structure is maintained. Such structure changes depend on the particle sizes, composition of the dope solution and the sintering temperature, which are discussed and presented in the following section.

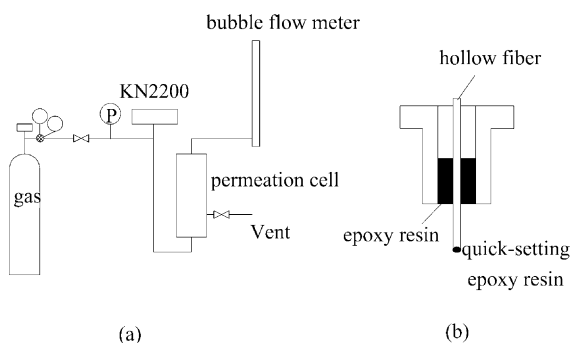


Fig. 1. The schematic diagram of apparatus for measuring gas permeation. (a) flow diagram; (b) permeation module.

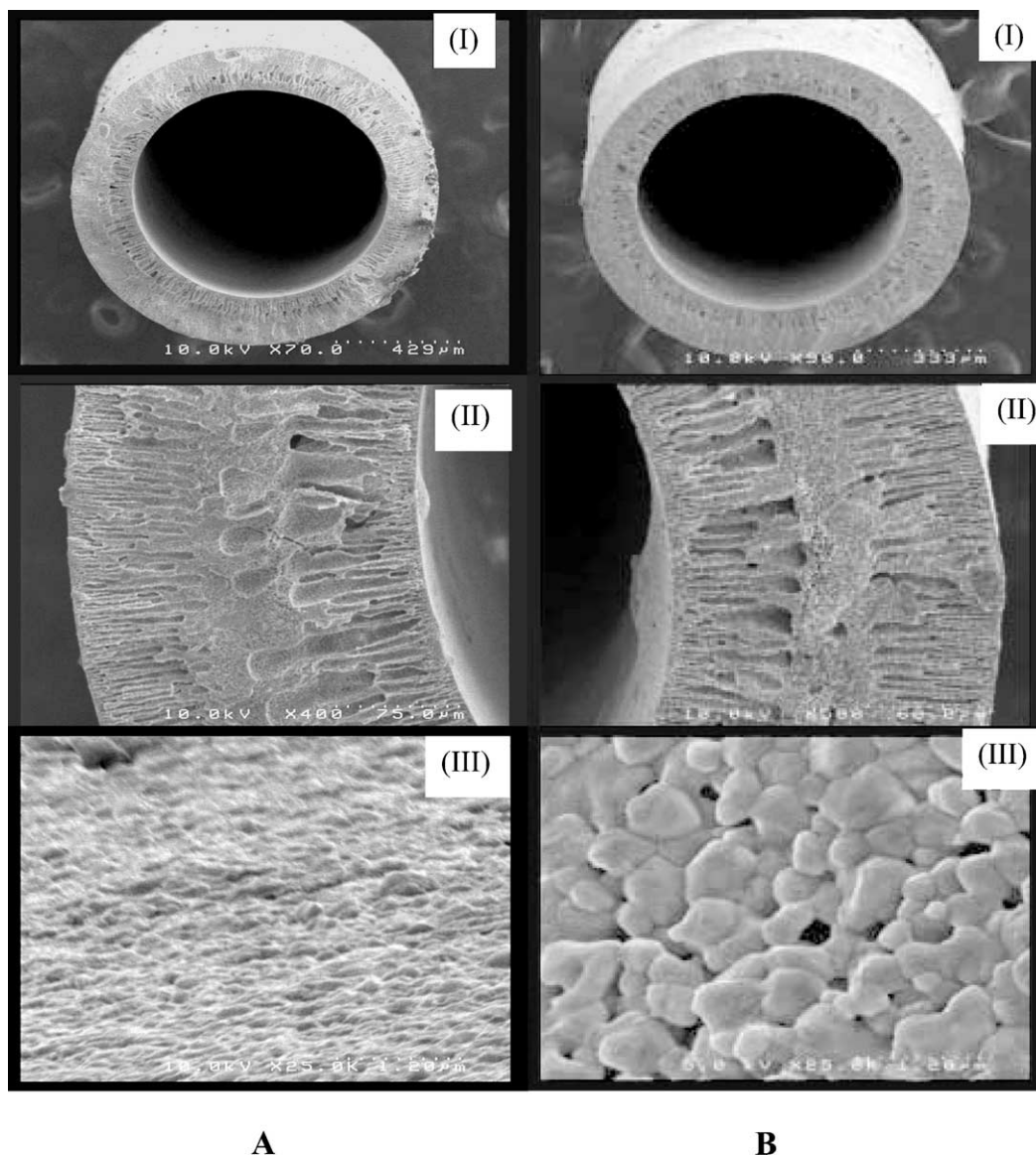


Fig. 2. SEM diagrams of the hollow fibres fabricated from the 1- $\mu\text{m}$   $\text{Al}_2\text{O}_3$  particles: A—before sintering; B—after sintering; (I) Overall view; (II) membrane walls; (III) membrane surfaces.

### 3.2. Physical properties of the $\text{Al}_2\text{O}_3$ hollow fibres

In practice, hollow fibre membranes are assembled as bundles in the module fabrication where a good mechanical strength of the hollow fibre membranes is usually required. Currently, ceramic hollow fibre membranes, in general, show a poor mechanical strength, which restricts its use in large-scale application. In this study, the mechanical strength of the  $\text{Al}_2\text{O}_3$  hollow fibre membranes prepared is dependant on several preparation and sintering conditions such as  $\text{Al}_2\text{O}_3$  particle size and its size distributions, the  $\text{Al}_2\text{O}_3$  content in the spinning dope, and sintering environment (i.e. sintering temperature and time), etc. In the following, the mechanical strength of the prepared hollow fibre membranes at different fabricating and sintering conditions is discussed.

#### 3.2.1. Effect of temperature

Experimental data for this effect is shown in Fig. 4 where the hollow fibre membrane was prepared from 0.3- $\mu\text{m}$  particles. It can be seen that an increase of sintering temperature would enhance the mechanical strength. For example, at temperatures of 1300 and 1550  $^{\circ}\text{C}$  sintered for 10 h, the three-point (3P) values are 20.9 and 80.9 MPa, respectively. When the sintering is less than 1500  $^{\circ}\text{C}$ , the 3P value is proportional to the sintering temperature. When the sintering temperature is greater than 1550  $^{\circ}\text{C}$ , the 3P value increases sharply as the sintering temperature is further increased. It, thus, suggests that preparation of the  $\text{Al}_2\text{O}_3$  hollow fibre membranes with high mechanical strength are possible at the sintering temperature of 1550  $^{\circ}\text{C}$  or higher, as a slight increase in temperature would dramatically



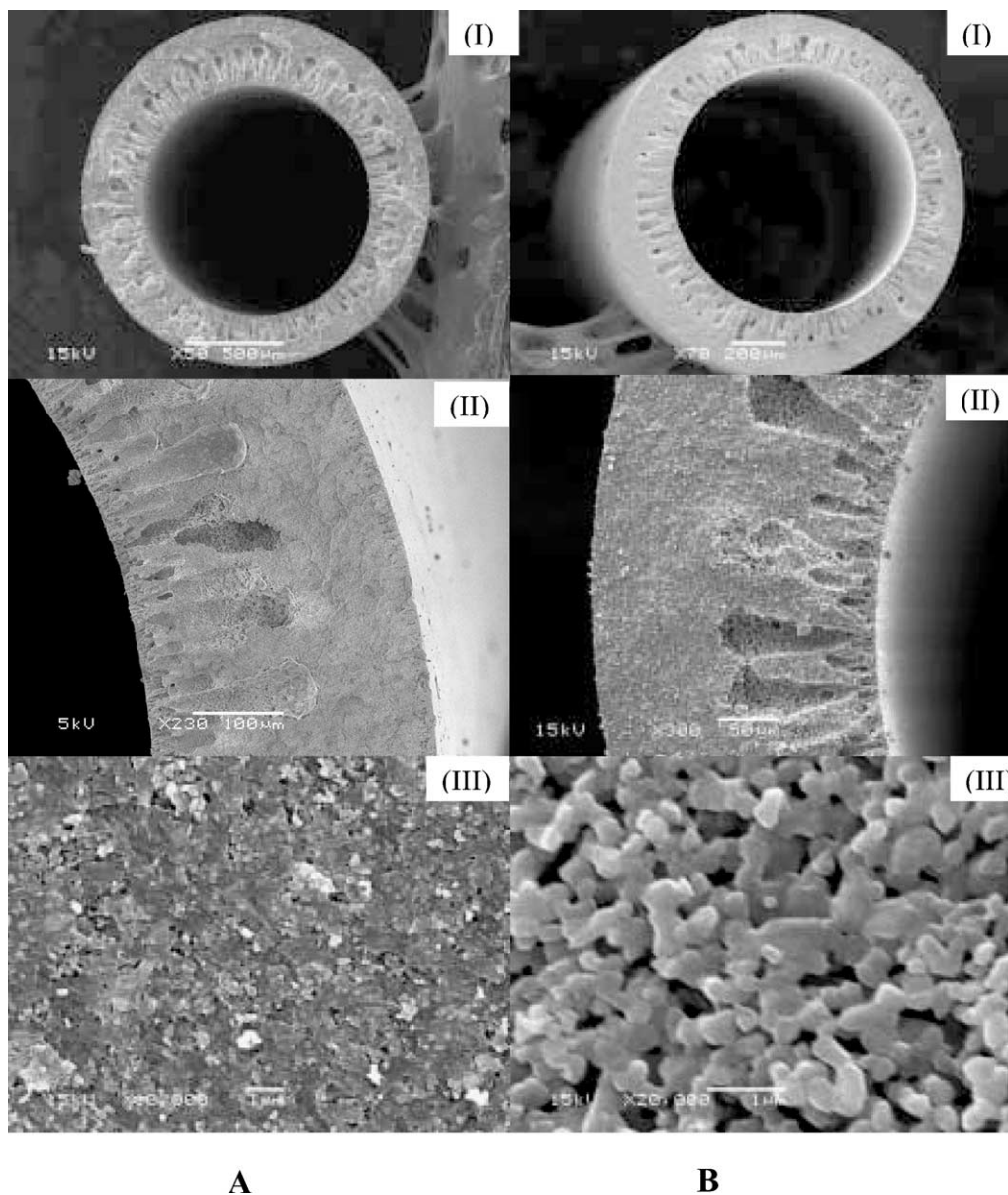


Fig. 3. SEM diagrams of the hollow fibres fabricated from the 0.3- $\mu\text{m}$   $\text{Al}_2\text{O}_3$  particles: A—before sintering; B—after sintering; (I) overall view; (II) membrane walls; (III) membrane surfaces.

increase the mechanical strength. Sintering of the hollow fibre at the temperature of 1600 °C shows, of course, the increase in the mechanical strength, however, gas permeability is decreased considerably as shown in Fig. 4. Therefore, there is a trade-off between the mechanical strength and gas permeability. The 3P values at various sintering temperatures suggest that the sintering temperature at 1550 °C would give sufficient strength for the fibre to be fabricated into a module without breaking.

### 3.2.2. Effect of the $\text{Al}_2\text{O}_3$ content

The hollow fibre precursor formed through the phase inversion techniques contains the  $\text{Al}_2\text{O}_3$  powder and the PESf binder. During the sintering process, the PESf is removed and the  $\text{Al}_2\text{O}_3$  hollow fibre is ultimately

formed. Therefore, the  $\text{Al}_2\text{O}_3$  content in the spinning dopes plays the important roles in determining its mechanical strength. Fig. 5 illustrates the effect of  $\text{Al}_2\text{O}_3$  content on the fibre mechanical strength and its gas permeability. It can be seen that the 3P value enhances greatly, as the  $\text{Al}_2\text{O}_3$ /PESf ratio is increased. Compared to the sintering temperature, the increase of the  $\text{Al}_2\text{O}_3$  powder content in the spinning dope would result in a much more obvious effect on the fibre mechanical strength. It, therefore, follows that in order to produce a  $\text{Al}_2\text{O}_3$  hollow fibre membrane with higher mechanical strength, the higher  $\text{Al}_2\text{O}_3$  content in the solution dope must be maintained. At  $\text{Al}_2\text{O}_3$ /PESf ratio of 7 or greater, reduction in gas permeability is tailed, indicating that the membrane is transformed to a much denser structure.

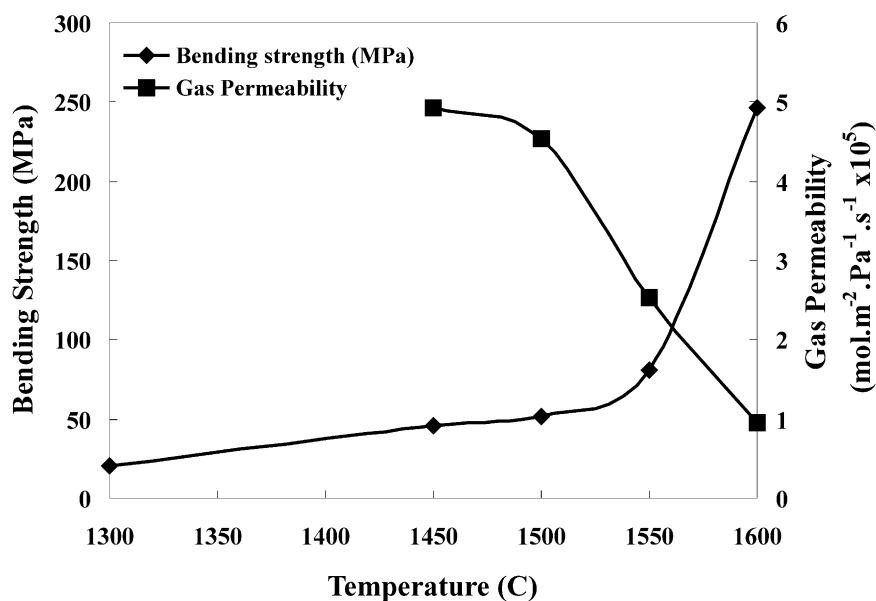


Fig. 4. Effect of sintering temperature on the mechanical strength and gas permeability of hollow fibre membranes prepared from 0.3- $\mu\text{m}$   $\text{Al}_2\text{O}_3$  powder at  $\text{Al}_2\text{O}_3/\text{PESf}$  ratio of 5; sintered for 10 h.

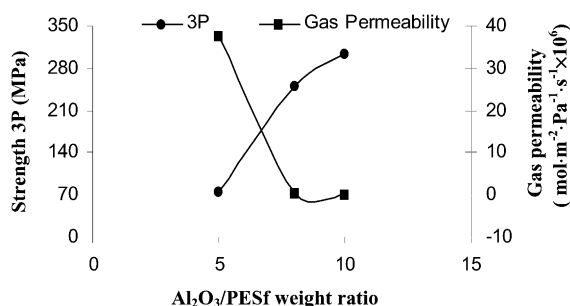


Fig. 5. Effect of  $\text{Al}_2\text{O}_3$  content on the mechanical strength and gas permeability of the hollow fibre membranes prepared from 1.0- $\mu\text{m}$   $\text{Al}_2\text{O}_3$  particles, sintering temperature of 1550 °C.

### 3.2.3. Effect of particle size and size distribution

Pores in the sintered ceramic hollow fibre membranes are voids left between packed particles, having neither a regular shape, nor a regular size. The particle size and size distribution of the  $\text{Al}_2\text{O}_3$  powders in the spinning dope plays an important role in determining the membrane wall density and gas permeability. It has been shown [14] that a higher  $\text{Al}_2\text{O}_3$  content in the solution dope would produce a denser membrane with a lower porosity and smaller pore size. When the  $\text{Al}_2\text{O}_3$  content is too high, it is difficult to form a hollow fibre precursor using the phase inversion process. The  $\text{Al}_2\text{O}_3/\text{PESf}$  ratio of 5 has, therefore, been suggested and employed in this

Table 1  
Experimental results

No.	$\text{Al}_2\text{O}_3$ powders 1/0.3/0.01( $\mu\text{m}$ )	Sintering temperature (°C)	Gas permeability mol $\text{m}^{-2}\text{Pa}^{-1}\text{s}^{-1}$ ( $\text{N}_2$ , 1 atm)	Bending strength $\sigma_F$ (MPa)
AI	100/0/0	1500	6.50E-5	48.6
BI	50/50/0	1500	3.90E-5	59.3
CI	0/100/0	1500	4.53E-5	51.3
DI	46.5/46.5/7	1500	2.78E-5	72.8
AII	100/0/0	1550	3.75E-5	76.1
BII	50/50/0	1550	3.59E-5	93.56
CII	0/100/0	1550	2.54E-5	80.9
DII	46.5/46.5/7	1550	1.60E-5	107
AIII	100/0/0	1600	1.15E-5	182.41
BIII	50/50/0	1600	0.98E-5	253.08
CIII	0/100/0	1600	0.95E-5	246.16
DIII	46.5/46.5/7	1600	0.22E-5	341.72

study for preparation of a  $\text{Al}_2\text{O}_3$  hollow fibre membrane with a meaningful mechanical strength and appreciable permeation characteristics using the dope solutions containing different sizes of the  $\text{Al}_2\text{O}_3$  powders. The experimental result is given in Table 1. It indicates that the gas permeability decreases and mechanical strength of the hollow fibre increase as the average particle size of the  $\text{Al}_2\text{O}_3$  powders is decreased. The results given in Table 1 clearly correspond with the SEM graphs presented earlier. Further comparison of the experimental results given in Fig. 5 and Table 1 reveals that blending the smaller  $\text{Al}_2\text{O}_3$  particles in the spinning solution is a more effective way in producing the  $\text{Al}_2\text{O}_3$  hollow fibre membrane with increased mechanical strength without considerably losing its permeation characteristics.

#### 4. Conclusions

A organic binder solution (dope) containing suspended aluminium oxide ( $\text{Al}_2\text{O}_3$ ) powders, either in mono size or a distributed size, is spun to a hollow fibre precursor, which is then sintered at elevated temperatures. The mechanical strength and gas permeability of the resulting membranes are determined and one of the most important fabrication parameters, i.e. choice of the starting  $\text{Al}_2\text{O}_3$  particle size in the spinning dope, is explored.

The prepared membranes have the asymmetric structure, i.e. the sponge-like structures coupled with the finger-like structures located at inner walls of the fibre. The sintered membranes show the different degrees of the shrinkage. Compared to the fibres prepared from 1- $\mu\text{m}$  particles, the fibre prepared from 0.3- $\mu\text{m}$  particles shows a much denser structure, which probably resulted from the higher shrinkage during the sintering process. Experimental results also revealed that  $\text{Al}_2\text{O}_3$  powders with a distributed particle size could be employed in producing the  $\text{Al}_2\text{O}_3$  hollow fibre membranes with high mechanical strength and appreciable gas permeation characteristics.

#### Acknowledgements

The authors gratefully acknowledge the research funding provided by EPSRC in the United Kingdom (grant No. GR/N38640).

#### References

- [1] Shaomin Liu, Xiaoyao Tan, K. Li, R. Hughes, Methane coupling using catalytic membrane reactors, *Cat. Rev. Sci. Eng.* 43 (2001) 147.
- [2] G. Saracco, G.F. Versteeg, W.P.M. van Swaaij, Current hurdles to the success of high-temperature membrane reactors, *J. Membrane Sci.* 95 (1994) 105.
- [3] H.P. Hsieh, Inorganic membrane reactors, *AIChE Symp. Ser.*, No. 268 (85) (1989) 53.
- [4] H.P. Hsieh, General characteristics of inorganic membranes, in: Ramesh R. Bhave (Ed.), *Book of Inorganic Membranes Synthesis, Characteristics and Applications*, 1991, pp. 65–93.
- [5] J.N. Armor, Applications of catalytic inorganic membrane reactors to refinery products, *J. Membrane Sci.* 147 (1998) 217.
- [6] R.A. Terpstra, J.P.G.M. Van Eijk, F.K. Feenstra, Method for the Production of Ceramic Hollow Fibres, US patent 5,707,584, 1998.
- [7] J. Smid, C.G. Avci, V. Günay, R.A. Terpstra, J.P.G.M. Van Eijk, Preparation and characterisation of microporous ceramic hollow fibre membranes, *J. Membrane Sci.* 112 (1996) 85.
- [8] H.W. Brinkman, J.P.G.M. Van Eijk, H.A. Meinema, R.A. Terpstra, Innovative hollow fiber ceramic membranes, *Am. Ceram. Soc. Bull.* (1999) 51.
- [9] R.A. Terpstra, J.P.G.M. Van Eijk, J.C.T. van der Heijde, Alternative way of producing silicon nitride ceramics for membrane application, *Key Eng. Mater.* 132–136 (1997) 1770.
- [10] K.H. Lee, Y.M. Kim, Asymmetric hollow inorganic membranes, *Key Eng. Mater.* 61 and 62 (1991) 17.
- [11] J.E. Koresch, A. Sofer, Molecular sieve carbon permselective membrane, Part I. Presentation of a new device for gas mixture separation, *Sep. Sci. Technol.* 18 (1983) 723.
- [12] J.E. Koresch, A. Sofer, Mechanism of permeation through molecular-sieve carbon membrane, *J. Chem. Soc., Faraday Trans.* 82 (1986) 2057.
- [13] V.M. Linkov, R.D. Sanderson, E.P. Jacobs, Highly asymmetrical carbon membranes, *Proc. 34th IUPAC Symp. Macromolecules* 7 (1992) 56.
- [14] X. Tan, S. Liu, K. Li, Preparation and characterization of inorganic hollow fibre membranes, *J. Membrane Sci.* 188 (2001) 87.
- [15] J. Luyten, A. Buekenhoudt, W. Adriansens, J. Cooymans, H. Weyten, F. Servaes, R. Leysen, Preparation of  $\text{LaSrCoFeO}_{3-x}$  membranes, *J. Membrane Sci.* 135 (2000) 637.
- [16] S. Liu, X. Tan, K. Li, R. Hughes, Preparation and characterisation of  $\text{SrCe}_{0.95}\text{Yb}_{0.05}\text{O}_{2.975}$  hollow fiber membranes, *J. Membrane Sci.* 193 (2001) 249.
- [17] J. J. Hammel, Porous Inorganic Siliceous-containing Gas Enriching Material and Process of Manufacture and Use, US patent 4,853,001, 1989.
- [18] S.P. Deshmukh, K. Li, Effect of ethanol composition in water coagulation bath on morphology of PVDF hollow fibre membranes, *J. Membrane Sci.* 150 (1998) 75.
- [19] J.N. Cernica, *Strength of Materials*, 2nd edition, Holt, Rinehart, and Winston, New York, 1977, p. 469.
- [20] J.B. Wachtman, *Mechanical Properties of Ceramics*, Wiley, New York, 1996, pp. 74–77.